

Dynamics of Contact Line Pinning in Capillary Rise and Fall

Erik Schäffer and Po-zen Wong

Department of Physics and Astronomy, University of Massachusetts, Amherst, Massachusetts 01003

(Received 18 September 1997)

The dynamics of water columns rising and falling in vertical glass capillaries are studied near the pinning threshold. In tubes with rough interior walls, the column height h as a function of time t exhibits stick-slip behavior. In tubes with smooth walls, falling experiments show no pinning effects, but rising experiments exhibit critical behavior with nonunique exponents. We argue that this is due to the fact that fluid has to be transported in a microscopic wetting film which does not have a stationary structure. Similar restrictions can affect avalanche dynamics in other systems. [S0031-9007(98)05750-0]

PACS numbers: 47.60.+i, 05.40.+j, 68.10.-m, 68.45.Gd

That raindrops stuck on the window can trickle down or stop at random times is an intriguing phenomenon. Qualitatively, it seems obvious that the air-water contact line is pinned by the random potential on the glass surface. We expect a drop to move when its weight exceeds the pinning force and to stop when it encounters stronger pinning forces. This kind of stick-slip behavior has been proposed as an essential feature of *dynamical critical phenomena* [1] in which a randomly pinned dynamical system driven by a force F can have an *average* velocity v that diminishes algebraically at a threshold F_c . Similar to equilibrium second-order phase transitions,

$$v = v_o(F/F_c - 1)^\beta, \quad (1)$$

where the exponent β exhibits universality. Microscopically, the system overcomes the pinning forces by discrete avalanches. The waiting time τ for an avalanche of size ξ obeys dynamic scaling: $\tau \propto \xi^z$. At the critical point F_c , both ξ and τ diverge, and the avalanche distribution follows an inverse power law. This generic picture has been suggested to apply to depinning transitions in a wide range of systems, including sliding charge-density waves [2], flux lattices in superconductors [3], magnetic domain walls [4], and fluid interfaces in porous media [5]. Although Eq. (1) often fits the data, the value of β never seems to agree between theory and experiment.

The depinning of contact lines is one of the best known cases to which Eq. (1) is often applied [6], but the value of β varies widely among studies using different fluids and substrates, and the cause is unclear [7]. There have also been many model calculations, but each employed different assumptions and predicted different values for β [6,8]. While experiments have all found $\beta > 1$ [7], theory based on the avalanche picture predicts $\beta < 1$ [9]. Thus the universality of the depinning transition remains an appealing but unproven idea. A summary of the experimental and theoretical situations is given elsewhere [10,11]. Here, we report an experiment which suggests that the avalanches are constrained by fluid transport in a wetting film. Similar effects in other systems may explain the apparent lack of universality.

In order to minimize chemical complications, we have chosen to study the vertical rise and fall of deionized water in cleaned glass capillaries, subjected only to the natural gravity, viscous, and interfacial forces. For tube radius r , the equilibrium height of the water column is given by $H_{eq} = 2\gamma \cos \theta / r\rho g$, where γ is the air-water surface tension, θ the contact angle, ρ the water density, and g the gravitational acceleration. With pinning effects, a rising column would stop at a height $H_c < H_{eq}$ and a falling column would have $H_c > H_{eq}$. Assuming a constant θ , the net *average* driving pressure on the water column at any height h is $P = \rho g(H_{eq} - h)$ and the threshold pinning pressure is $P_c = \rho g(H_{eq} - H_c) \equiv \rho g H_{gap}$. Thus Eq. (1) can be expressed as

$$\frac{dh}{dt} = v_o \left(\frac{H_c - h}{H_{gap}} \right)^\beta. \quad (2)$$

This is appropriate provided the flow rate is sufficiently low so that the viscous pressure drop is negligible. Integrating from initial time t_1 and height h_1 gives for $\beta \neq 1$,

$$h(t) = H_c - (H_c - h_1)[1 + A(t - t_1)]^{1/(1-\beta)}, \quad (3)$$

where $A = (\beta - 1)v_o(H_c - h_1)^{\beta-1}/H_{gap}^\beta$. This solution has the feature that if $\beta < 1$, h stops at H_c after a finite time given by $t = t_1 - 1/A$. If $\beta > 1$, h approaches H_c algebraically as $t \rightarrow \infty$. If $\beta = 1$, Eq. (2) has an exponential solution,

$$h(t) = H_c - (H_c - h_1)e^{-(t-t_1)/\tau_1}, \quad (4)$$

where $\tau_1 = H_{gap}/v_o$. Thus β can be determined by measuring $h(t)$ in capillary rise and fall. This method has the advantage that a wide range of velocity can be covered without employing any mechanical driving device, so the contact line approaches criticality in a self-organized manner. It had been used previously to study the pinning of fluid interfaces in porous media [5]. The results show that β was highly irreproducible but always greater than

unity. One possible explanation is that the fluid interface intersects the porous media by many contact lines and each has complicated pinning dynamics. Carrying out a similar study for a single contact line allows us to track down the cause of this peculiar behavior and also probe the effects of dimensionality in depinning transitions. Since both rise and fall experiments can be performed in the same tube, the gap between their final heights is a useful indicator of the pinning strength F_c as well as the size of the critical region. This reduces the uncertainties in the data analyses.

Two different types of capillaries were used in our study, one with rough interior walls and the other with smooth walls, both made of the same borosilicate low expansion glass (Corning code 7740). They are designated as R tubes and S tubes, respectively. Figure 1 shows the difference in wall roughness as revealed by a scanning electron microscope. The tubes were cleaned by first flowing 400 ml of 1 M hydrochloric acid through them in one hour, followed by an equal amount of deionized water, and then boiling them in deionized water for eight hours. They were placed in the apparatus immediately after cleaning. This procedure substantially reduced the uncontrolled chemical heterogeneities on the surface. As the data show, surface roughness is the dominant cause of pinning. For each type of tubes, several tube diameters were studied: 250, 310, and 410 μm for R tubes; 180, 200, 250, 300, and 355 μm for S tubes. For each size, several samples were used.

The apparatus is similar in concept to that used by Delker *et al.* [5] but different in many details. The capillary stands vertically in a large beaker containing water. The top of the tube is connected to a three-way valve that switches to either a 100% humidity chamber at ambient pressure or to a plastic syringe. The syringe is used to raise or lower the water column to set the initial position of the meniscus. Switching the connection to ambient pressure lets the meniscus move according to the natural forces present. The humidity chamber ensures that the meniscus position is unaffected by evaporation. To observe the delicate motion near the pinning threshold, a small inspection microscope is oriented to view horizontally. A video camera attached to it captures the image of the meniscus which is

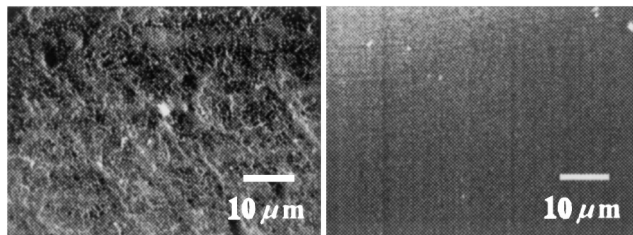


FIG. 1. Scanning electron micrographs show that the R tubes have rough interior walls and the S tubes have smooth walls. The white spots in the images are particles used to mark the location and not parts of the surface.

illuminated from the bottom of the beaker by a fiber optic lamp. The images are digitized by a microcomputer at set time intervals. Gray-scale thresholding and edge detection algorithms are used to determine the shape of the meniscus from which its average height $h'(t)$ in the frame is computed. The image field is about 3.5 mm and spans 640 pixels; hence the resolution is about 5.5 $\mu\text{m}/\text{pixel}$. Since the column height is of the order of 10 cm and the air-water surface tension changes by about 0.2% K, the apparatus was placed in a temperature controlled and thermally insulated box. Only the manual syringe and the power supply of the lamp are outside the box. The temperature stability is better than ± 10 mK over a two-hour period. Each run lasted no more than 15 min and the temperature variation was within ± 4 mK, which affects the meniscus position by about 1 μm (~ 0.2 pixel). Data far from the threshold were also taken, using a wide-angle 8 mm camera lens instead of the microscope. A 14 cm field of view could be captured. Combining the two arrangements, the velocity data ranges from 10^{-2} to 10^4 $\mu\text{m}/\text{s}$. At the fast end, viscous damping is more important than the fluctuations in interfacial forces and the dynamics is described by the well known Washburn equation [5,12]. It predicts an exponential approach to the equilibrium height H_{eq} with a time constant

$$\tau_w \equiv 8(h_o + H_{\text{eq}})\eta/\rho g r^2, \quad (5)$$

where η is the viscosity and h_o is the length of the tube immersed in water. The capillary number Ca , defined as $\eta v/\gamma$, is a measure of the relative strength of viscous and interfacial forces. The range in this study, $10^{-10} < \text{Ca} < 10^{-4}$, is wider and lower than any previous study.

Figure 2(a) shows the rise and fall $h(t)$ data taken with a 250 μm diameter S tube on a coarse scale. The solid lines are fits to the Washburn equation. The two fitting parameters H_{eq} and τ_w obtained from the rise and fall data are in reasonable agreement. Calculating them using the known experimental parameters and assuming $\theta = 0^\circ$ gave similar values. Small differences can be attributed to the fact that θ is nonzero, velocity dependent, and exhibits hysteresis between advancing (rise) and receding (fall) experiments [13]. Thus, there appears to be no evidence of pinning. However, the magnified scale in the inset shows that there is actually a gap of about 1 mm between the rise and fall after 50 s. This gap is due to the fact that the tube was not used immediately after cleaning. The surface was contaminated simply by exposure to air. In contrast, Fig. 2(b) shows the high resolution data obtained in a properly cleaned and handled 180 μm S tube. h' is the relative position within the viewing frame (differs from h by a constant) and it shows a gap of about 10 μm . We note that the Washburn equation fits the falling data completely and τ_w agrees within 2% with the values obtained from the coarse scale data and that calculated from Eq. (5). The final height H'_{eq} within the frame is reproducible within 0.5 pixel. Thus, the falling

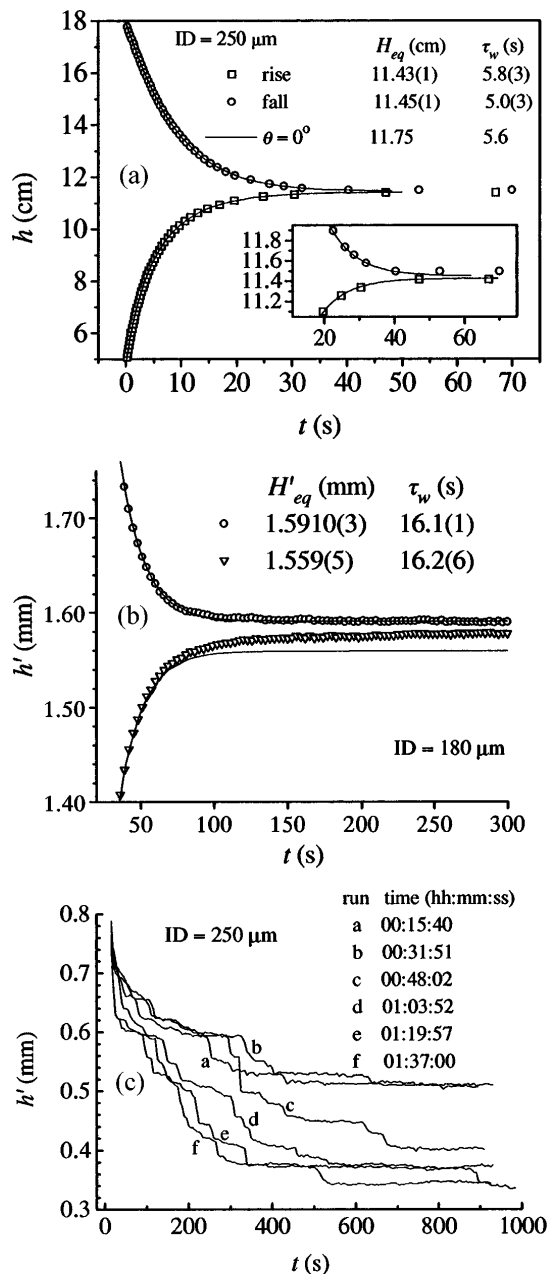


FIG. 2. Examples of capillary rise and fall data observed in different tubes with different resolutions. (a) Coarse resolution $h(t)$ data from a slightly contaminated 250 μm diameter S tube. (b) High resolution data from a properly cleaned 180 μm diameter S tube. h' and H'_{eq} are the heights within the viewing frame and not the true height. (c) High resolution falling data from a 250 μm diameter R tube show stick-slip behavior. See text for details.

data show no evidence of pinning and lend confidence that the tubes are sufficiently clean. However, the rising data in Fig. 2(b) do deviate from the Washburn fit at late times. Fitting them to Eq. (3) gives $\beta = 1.39$ [Fig. 3(a)], which suggests that pinning effects are present. This contrast between the rise and fall data holds true for all the S tubes, but the values of β vary between 1.1 and 4 [10,11].

For the R tubes, the coarse scale data are similar to Fig. 2(a) and they fit the Washburn equation well. However, the high resolution data in the pinning region are different. Figure 2(c) shows several sets of falling data obtained consecutively in a 250 μm R tube. Each run lasted about 15 min and the starting times are indicated. They clearly show stick-slip dynamics as predicted by the theories. We did not attempt to determine the avalanche size distribution, in part because of inadequate resolution in measuring the size, but also because the events are correlated among different runs in the same tube. It is unfeasible to study a large number of tubes. We note, for example, every run in Fig. 3 shows sticking at $h' \approx 0.6$ mm. However, the time it took to overcome the pinning is random [14]. This implies that background noise and the history of the system affect the dynamics. In addition, since discrete movement of the entire meniscus is observed, it means that the correlation length exceeds the system size ($\xi \sim r$); thus fitting the data to Eq. (3) would be inappropriate. Such analyses are valid only when small parts of the contact line undergo discrete jumps while the average position of the line appears to change smoothly. In other words, the roughness in the R tubes is too large and the observed behavior reflects finite-size effects. In the S tubes, the surface roughness is extremely weak. The disorder may be shielded from the contact line by a wetting film during the fall experiment, but weakly exposed in the rise experiment after the wetting film became thinner.

To test the above explanation, we performed repetitive runs by varying the waiting time (Δt) between consecutive runs. Since the structure of the wetting film is expected to change during Δt , it should affect the data. We found that the falling data were reproducible to ± 0.5 pixel, within experimental tolerance. Fits to Eq. (4) also resulted in parameters (H_c, τ_1) that agreed with (H_{eq}, τ_w) obtained from Washburn analyses of the coarse scale data. In contrast, the rise data were never reproducible. Figure 3(a) shows that the rise is generally slower with increased Δt , which corresponds to a larger β . In each run, we used the syringe to first raise the meniscus above H'_{eq} , then push it down outside the image field and wait before the start of a rise experiment. Δt is measured from the moment the meniscus passes H'_{eq} on its way down and the moment it reenters the frame on its way up. It gives a rough measure of the total time available for the wetting film to reorganize. The typical quality of the fits are depicted in Fig. 3(b) where the velocity $v = dh'/dt$ is plotted against the reduced driving force $f \equiv (H'_c - h')/H_{gap}$ on a log-log scale. We note that the power-law behavior was observed over two to three decades in v or Ca . When β is close to unity, this corresponds to a similar range in f . For larger β , the range in f is reduced. These results indicate that there are changes in the system that affect the advancing contact line in capillary rise and the most logical candidate is the wetting film on the surface. Clearly, when the film has more time to reorganize, the more it would expose the surface

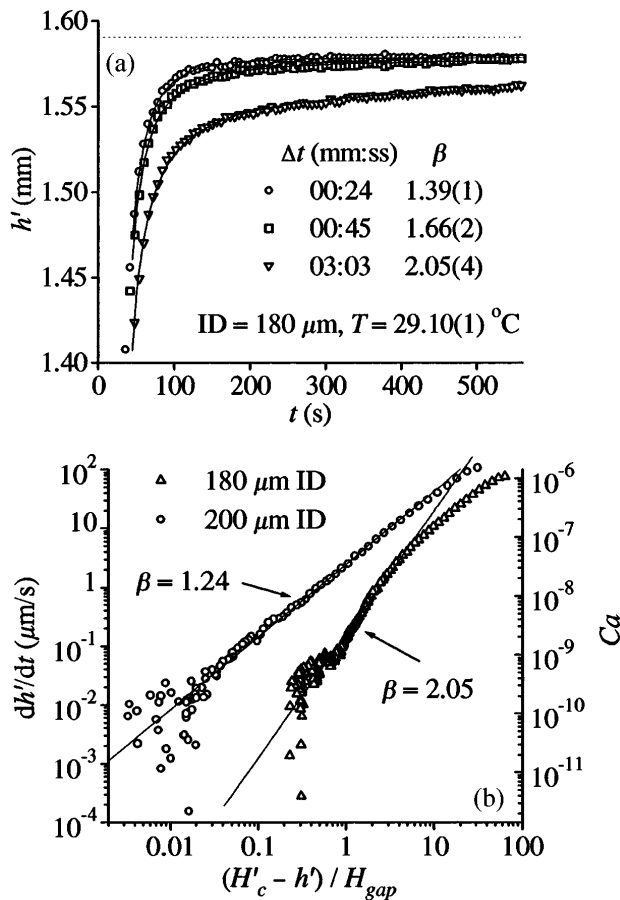


FIG. 3. Using Eq. (3) to fit the capillary rise data in S tubes results in different values of β . (a) In the same tube, β generally increases with longer waiting time Δt . (b) Among different tubes, although β varies, the power-law behavior spans two to three decades in v or Ca . The upper limit of the reduced driving force is consistently at $(H'_c - h')/H_{\text{gap}} \approx 4$.

roughness. Whether the physical changes are discrete molecular movements or continuous draining of the film is beyond our detection.

From the above results, one may be inclined to conclude that Eq. (1) or (2) is purely empirical and the exponent β bears no special meaning, but there is also evidence to the contrary. In Fig. 3(b) and similar plots of our data, we found that the upper limit of power-law behavior consistently occurs at a reduced driving force $f \approx 4$. We also found that the parameter $v_o \propto H_{\text{gap}}^3$ applies to all our data [10,11]. These are unlikely to be random coincidences. A more logical view is that while the concept of avalanches is important to the depinning of contact lines, a full understanding should take into account the effects of the wetting film. When the liquids and solid substrates are changed, or when the temperatures and velocities vary, the nature of the film is altered and the data can become irreproducible. This would explain why every contact line experiment seems to find different values for β . This is actually *not* surprising because, in molecular dynamics simulations, it has been shown that the no-slip bound-

ary condition breaks down at the contact line within two atomic layers [15]. In studies of liquid drop spreading, both simulations [16] and experiments [17] have found that molecular layers spread in advance of the bulk fluid. Hence, we would expect the avalanche dynamics to be intimately coupled to how fluid is transported near the contact line and in the wetting film. Extending this conclusion to other physical systems, we note that *conservation laws* are expected to affect critical dynamics. Avalanches of fluids and sandpiles are constrained by mass conservation and the details of mass transport, while domain wall motion in a magnet has no such constraints [5]. Grinstein and others have analyzed the effects of conservation laws in the context of self-organized critical phenomena [18]. It would be interesting if similar considerations, taking into account the details of the transport mechanisms, can be given to depinning transitions in different physical systems.

We thank D.J. Durian, J. Machta and M.O. Robbins for helpful discussions. This work is supported by NSF Grant No. DMR-9404672.

- [1] J. Koplik and H. Levine, Phys. Rev. B **32**, 280 (1985); C. Tang and P. Bak, Phys. Rev. Lett. **60**, 2347 (1988); T. Nattermann *et al.*, J. Phys. II (France) **2**, 1483 (1992); O. Narayan and D.S. Fisher, Phys. Rev. B **48**, 7030 (1993).
- [2] M. Higgin, A.A. Middleton, and S. Bhattacharya, Phys. Rev. Lett. **70**, 3784 (1993).
- [3] S. Bhattacharya and M.J. Higgins, Phys. Rev. Lett. **70**, 2617 (1993); M.C. Hellerqvist, D. Ephron, W.R. White, M.R. Beasley, and A. Kapitulnik, *ibid.* **76**, 4022 (1996).
- [4] P.-z. Wong and J.W. Cable, Phys. Rev. B **28**, 5361 (1983); J.S. Urbach, R.C. Madison, and J.T. Markert, Phys. Rev. Lett. **75**, 276 (1995).
- [5] T. Delker, D.B. Pengra, and P.-z. Wong, Phys. Rev. Lett. **76**, 2902 (1996); J.P. Stokes, A.P. Kushnick, and M.O. Robbins, *ibid.* **60**, 1386 (1988).
- [6] E. Raphaël and P.G. de Gennes, J. Chem. Phys. **90**, 7577 (1989); J.F. Joanny and M.O. Robbins, *ibid.* **92**, 3206 (1990).
- [7] See, e.g., S. Kumar, D.H. Reich, and M.O. Robbins, Phys. Rev. E **52**, R5776 (1995), and references therein.
- [8] P. Sheng and M. Zhou, Phys. Rev. A **45**, 5694 (1992).
- [9] D. Ertas and M. Kardar, Phys. Rev. E **49**, R2532 (1994).
- [10] E. Schäffer, Master's thesis, University of Massachusetts, Amherst, 1997.
- [11] E. Schäffer and P.-z. Wong (to be published).
- [12] E.W. Washburn, Phys. Rev. **17**, 273 (1921).
- [13] See, e.g., *Contact Angle, Wettability and Adhesion*, edited by F.M. Fowkes (American Chemical Society, Washington, DC, 1964).
- [14] G.D. Nadkarni and S. Garoff, Langmuir **10**, 1618 (1994).
- [15] P.A. Thompson and M.O. Robbins, Phys. Rev. Lett. **63**, 766 (1989).
- [16] J.-x. Yang, J. Koplik, and J.R. Banavar, Phys. Rev. Lett. **67**, 3639 (1991).
- [17] A.-M. Cazabat, Contemp. Phys. **28**, 347 (1987).
- [18] G. Grinstein, J. Appl. Phys. **69**, 5441 (1991).